Effect of n-p-n heterostructures on interface recombination and semiconductor laser cooling

G. Rupper,[1] N. H. Kwong,[1,2] R. Binder,[1,3,a)] Ch.-Y. Li,[4] and M. Sheik-Bahae[4]
[1]*College of Optical Sciences, University of Arizona, Tucson, Arizona 85721, USA*
[2]*Department of Physics, Centre for Optical Sciences, The Chinese University of Hong Kong, Hong Kong, People's Republic of China*
[3]*Department of Physics, University of Arizona, Tucson, Arizona 85721, USA*
[4]*Department of Physics and Astronomy, Optical Science and Engineering, University of New Mexico, Albuquerque, New Mexico 87131, USA*

(Received 26 August 2010; accepted 19 October 2010; published online 13 December 2010)

The design of doped n-p-n semiconductor heterostructures has a significant influence on the structures' nonradiative decay and can also affect their photoluminescence characteristics. Such structures have recently been explored in the context of semiconductor laser cooling. We present a theoretical analysis of optically excited n-p-n structures, focusing mainly on the influence of the layer thicknesses and doping concentrations on nonradiative interface recombination. We find that high levels of n-doping (10^{19} cm^{-3}) can reduce the minority-carrier density at the interface and increase the nonradiative lifetime. We calculate time-dependent luminescence decay and find them to be in good agreement with experiment for temperatures >120 K, which is the temperature range in which our model assumptions are expected to be valid. A theoretical analysis of the cooling characteristics of n-p-n structures elucidates the interplay of nonradiative, radiative, and Auger recombination processes. We show that at high optical excitation densities, which are necessary for cooling, the undesired nonradiative interface recombination rates for moderate (10^{17} cm^{-3}) n-doping concentrations are drastically increased, which may be a major hindrance in the observation of laser cooling of semiconductors. On the other hand, high n-doping concentrations are found to alleviate the problem of increased nonradiative rates at high excitation densities, and for the model parameters used in the calculation we find positive cooling efficiencies over a wide range of excitation densities. © *2010 American Institute of Physics*. [doi:10.1063/1.3517144]

I. INTRODUCTION

Doped semiconductor heterostructures such as n-p-n junctions are ubiquitous in electronics and are of increasing importance on optoelectronics. While most of the electric transport issues are well understood, the optical properties and the nonradiative recombination of these systems are still the topic of current research. One example of an optoelectronic device that is currently being developed and whose optical properties are not well understood is an semiconductor-based all-optical cooler (for a recent overviews on optical refrigeration of solids see Refs. 1–3). The cooling principle is based on the absorption of an external laser beam, followed by frequency-upconversion (via phonon scattering) and high-frequency photoluminescence that carries more energy per photon out of the semiconductor than was deposited by the external light beam. The energy extraction can in principle lead to cooling of the semiconductor. It is hoped that in the future, semiconductor laser cooling can be achieved and compete with laser cooling of doped glass, where cryogenic temperatures have already been reached.[4]

Ideally, these devices contain only a simple piece of bulk semiconductor (e.g., GaAs) and some components that facilitate the extraction of photoluminescence light. In practice, however, that piece of GaAs is sandwiched between doped passivation layers (for example, GaInP), which serve to reduce the nonradiative recombination at the sample's main surfaces. Also, the active GaAs layer, though ideally undoped, is often unintentionally doped. For example, we have experimentally studied structures that included unintentionally p-doped GaAs layers (for example due to carbon impurities) and n-doped (with silicon) GaInP passivation layers.[5] We found one structure to have a very long nonradiative lifetime of 27 μs at room temperature, which is a promising result in terms of the prospects for cooling applications in which nonradiative decay is undesirable. While the benefits of the n-doped passivation layers are clearly established, the samples have not allowed for the observation of net cooling.

The aim of this paper is to provide a theoretical analysis that helps to design future generations of semiconductor structures with improved prospects for achieving laser cooling. In particular, we address the question of nonradiative lifetime in passivated GaAs structures and its dependence on the external laser intensity. In cooling applications, the pump creates relatively high concentrations of photoexcited carriers, while typical measurements of nonradiative lifetimes are performed at low densities of photoexcited carriers. Our analysis, and our proposals to further improve the design of n-p-n structures, is based on the assumption that most of the nonradiative decay processes happen at the GaAs/GaInP interface, as is expected for high-quality samples.[6] We will

a)Electronic mail: binder@optics.arizona.edu.

 © 2010 American Institute of Physics

Author complimentary copy. Redistribution subject to AIP license or copyright, see http://jap.aip.org/jap/copyright.jsp

analyze the effects of the n-p-n structure on the spatial carrier density profiles and on the nonradiative recombination at the interfaces.

The paper is organized as follows. In Sec. II, we outline our approach to the calculation of carrier density profiles in the n-p-n structure. In Sec. III we give a brief review of interface recombination concepts inasmuch they have some bearing on our present work. In Sec. IV we define and discuss a simple model for the nonradiative lifetime. Though not being used in our cooling analysis, this model helps us understand and interpret the results of the cooling study. In Sec. V we formulate a time-dependent theory to model the luminescence decay from n-p-n structure and compare the theoretical results with our experimental results obtained on two samples for different GaAs layer thickness. Finally, we present theoretical results for the cooling characteristics (in particular the cooling efficiency) of various n-p-n structures. Based on that analysis, we formulate a proposal for future generations of n-p-n structures that we believe would exhibit superior nonradiative recombination characteristics.

II. QUASITHERMAL HETEROSTRUCTURE THEORY

The heterostructure system is modeled assuming that the system is in quasithermal equilibrium, and that the overall system is charge neutral. Our analysis is similar to the analysis for total thermal equilibrium given in Ref. 7. The main difference between thermal equilibrium used in Ref. 7 and quasithermal equilibrium used in the following is the fact that we allow for optically created electrons and holes. In a quasithermal equilibrium state, the electron and the hole populations are thermalized with each other under the constraint that they do not recombine. Generally such a state for a two-band model is determined by three thermodynamics parameters: the temperature, the electron chemical potential, and the hole chemical potential. The assumption of overall charge neutrality imposes one condition on the three parameters so that only two can be independently set. The quasiequilibrium assumption is valid if the thermalization rate to this state is much faster than the recombination rate. This condition is met for temperatures below the band gap but not too low and for not too low densities.

The structure's geometry is a symmetrical n-p-n structure with a GaAs layer sandwiched between two GaInP passivation layers, see Fig. 1. In quasithermal equilibrium, the electron (n_e) and hole (n_h) densities in a free carrier model at any point in the system are given by:

$$n_{e/h}(z) = \frac{2}{L^3}\sum_{\mathbf{k}} \frac{1}{1 + e^{\beta[\epsilon_{e/h}(k) \mp eV(z) - \mu_{e/h} \pm E_{c/v}(z)]}}, \qquad (1)$$

where the inverse temperature is $\beta = 1/k_B T$, $\epsilon_{e(h)}(k) = (\hbar^2 k^2/2m_{e(h)})$, $V(z)$ is the electrical potential at point z, $\mu_e(\mu_h)$ is the chemical potential for the electrons (holes), $E_{c(v)}$ is the energy level of the conduction (valence) band edge. The factor of 2 in front of the wave vector sums is due to spin degeneracy. This degeneracy is exact for the conduction band, while for the valence band it is a model assumption neglecting the light hole band. In total thermal equilibrium, one would have the additional condition $\mu_e = -\mu_h$.

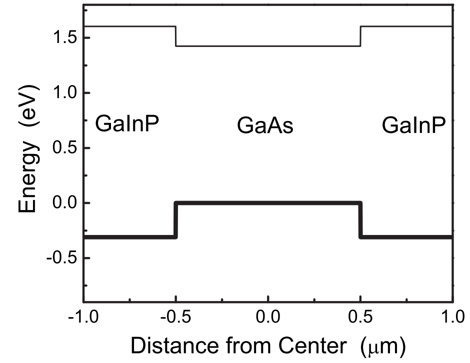

FIG. 1. Reference band structure at temperature $T = 300$ K before carriers are allowed to move. Conduction band (thin line), valence band (thick line). The thickness of the active layer (GaAs) in this example is 1 μm, and the passivation layers are 0.5 μm thick. Placing the center of the structure at $Z_c = 0$, the position of the junction is $Z_j = \pm 0.5$ μm, and the edge of the sample is $Z_e = \pm 1$ μm.

The density of ionized acceptors (donors) is given by:

$$N_a^-(z) = N_a\left\{1 - \frac{1}{1 + \frac{1}{D_a} e^{\beta[\epsilon_a + eV(z) - \mu_h - E_v(z)]}}\right\}, \qquad (2)$$

$$N_d^+(z) = N_d\left\{1 - \frac{1}{1 + \frac{1}{D_d} e^{\beta[\epsilon_d - eV(z) - \mu_e + E_c(z)]}}\right\}, \qquad (3)$$

where $N_a(N_d)$ is the density of acceptor (donor) sites, $D_a(D_d)$ is the degeneracy of the acceptor (donor) states, and $\epsilon_a(\epsilon_d)$ is the energy level of the acceptor (donor) state measured from the respective band edges.

The electrical potential is calculated from Poisson's equation. We assume that there is no external electrical field outside the semiconductor $[E(Z_e) = 0]$. The reference point for the electrical potential can be chosen arbitrarily. Due to the symmetry of the heterostructure, the middle of the structure is chosen as the reference point for the electrical potential, as well as the origin for the z-axis $[V(z=0) = 0]$. With this convention, the electric field in the GaInP passivation layer is given as:

$$E(z) = \frac{-4\pi e}{\epsilon_{\mathrm{GaInP}}}\int_{Z_e}^{z} dz' n_{\mathrm{charge}}(z'). \qquad (4)$$

For the GaAs layer, formally the same expression holds with $\epsilon_{\mathrm{GaInP}}$ replaced by ϵ_{GaAs}. Here, $n_{\mathrm{charge}}(z) = [n_e(z) - N_d^+(z)] - [n_h(z) - N_a^-(z)]$, Z_j is the position of the junction between GaAs and GaInP, Z_e is the position of the edge of the sample, $\epsilon_{\mathrm{GaInP}}$ is the dielectric constant of GaInP and ϵ_{GaAs} is the dielectric constant of GaAs. The electric potential is then given by $V(z) = -\int_0^z dz' E(z')$, and we assume total charge neutrality, $\int_{-Z_e}^{Z_e} dz n_{\mathrm{charge}}(z) = 0$.

As mentioned above, for a system in quasithermal equilibrium, its state can be specified by two parameters, which we choose to be the temperature and a density parameter. For the density parameter we choose to use the density of the minority carrier at the center of the semiconductor $[n_{\min}(z=0)]$, where $n_{\min}(z) = \min\{n_e(z), n_h(z)\}$.

Author complimentary copy. Redistribution subject to AIP license or copyright, see http://jap.aip.org/jap/copyright.jsp

In the description that follows, we solve Eqs. (1)–(4) selfconsistently.

Due to the symmetry of the system, only half of the structure needs to be modeled.

For the analysis we use the following parameters. The active GaAs layer thickness is either $d=0.75\ \mu$m or $d=1\ \mu$m. The GaAs is p-doped with either $N_a=10^{14}\ \mathrm{cm}^{-3}$ or $N_a=3.5\times10^{15}\ \mathrm{cm}^{-3}$. The GaAs is passivated by two n-doped GaInP layers with either $N_d=10^{17}\ \mathrm{cm}^{-3}$ or $N_d=10^{19}\ \mathrm{cm}^{-3}$. For GaAs, we use $E_g(T)=1520$ meV $-0.56[T^2/(T+226\ \mathrm{K})]$ meV/K, $m_e=0.067m_0$, and $m_h=0.48m_0$ where m_0 is the electron mass in vacuum. For GaInP we use $E_g=1.91$ at $T=300$ K, $m_e=0.105m_0$,[8] and $m_h=0.62m_0$.[9] Between the GaInP and GaAs we use a conduction band offset (CBO) of CBO=0.18 eV and a valence band offset (VBO) of VBO=0.31 eV, see pp. 5857–5858 of Ref.10. In our calculation, the CBO and VBO are independent of temperature which results in the GaInP $E_g=2.01$ eV at low temperature, which is within reported values. The acceptors are assumed to have a degeneracy factor of $D_a=4$ and the donors $D_d=2$.

III. INTERFACE RECOMBINATION IN HETEROSTRUCTURES

The main reason for adding an n-doped GaInP layer and creating an n-p-n heterostructure is to reduce the nonradiative surface recombination and thus to make optical refrigeration more easily achievable. But even if the surface recombination can be completely eliminated with the help of passivation layers, the interfaces between the active region and the passivation layers provide a channel for nonradiative recombination and thus need to be taken into account in a theory of luminescence and optical refrigeration. In this section, we will briefly review standard theoretical approaches to interface recombination.

The interface recombination is usually modeled with the use of the surface (or interface) recombination velocity (S). In terms of S, the surface recombination rate (U_s) is given by

$$U_s = Sn, \tag{5}$$

where n is the density of the minority carrier at the edge of the depletion region. In our case, the depletion region may extend all the way through the GaAs active region. If the active layer is sufficiently wide, the depletion region does not extend all the way through the active region. In this case, the density at the edge of the depletion region will be the same as the density at the center of the active region, and in our notation

$$U_s = Sn_{\min}(Z_c). \tag{6}$$

As pointed out in Refs. 11 and 12 the surface recombination velocity defined in this fashion is not a constant of the material and can be highly sensitive to the carrier densities. Using a Shockley-Read-Hall recombination model, the surface recombination can be modeled as[12]

$$U_s = \int_{E_v}^{E_c} \frac{\sigma_n\sigma_p\nu_{th,n}\nu_{th,p}[n_h(Z_j)n_e(Z_j)-n_i^2]N_{ss}(E)}{\sigma_n\nu_{th,n}[n_e(Z_j)+n_1]+\sigma_p\nu_{th,p}[n_h(Z_j)+p_1]}dE, \tag{7}$$

where $\sigma_n(\sigma_p)$ is the electron (hole) surface state capture cross sections, $\nu_{th,n}(\nu_{th,p})$ the electron (hole) thermal velocity, $n_e(Z_j)[n_h(Z_j)]$ the electron (hole) density at the surface, n_i the intrinsic density of the semiconductor, $N_{ss}(E)$ the density of surface states, $n_1=N_c e^{-\beta(E_c-E)}$, and $p_1=N_v e^{-\beta(E-E_v)}$.

To gain a better understanding of the general behavior of the surface recombination, we will follow the analysis of Correig *et al.*[11] and assume $\sigma_n=\sigma_p=\sigma$, $\nu_{th,n}=\nu_{th,p}=\nu_{th}$, and $N_{ss}(E)=N_{ss,0}\delta(E-E_f)$ where E_f is the Fermi level of an intrinsic semiconductor. Under these assumptions, Eq. (7) reduces to

$$U_s \approx \sigma\nu_{th}N_{ss,0}\frac{n_e(Z_j)n_h(Z_j)-n_i^2}{[n_e(Z_j)+n_i]+[n_h(Z_j)+n_i]}. \tag{8}$$

We now define a surface density surface recombination velocity $S_s=\sigma\nu_{th}N_{ss,0}$. With optical excitation, $n_e(Z_j)\gg n_i$ and/or $n_h(Z_j)\gg n_i$, the equation can be reduced to

$$U_s \approx S_s\frac{n_e(Z_j)n_h(Z_j)}{n_e(Z_j)+n_h(Z_j)}. \tag{9}$$

We note that if one of the densities is significantly larger than the other, the surface recombination becomes

$$U_s \approx S_s \min\{n_e(Z_j),n_h(Z_j)\} \equiv S_s n_{\min}(Z_j), \tag{10}$$

which is essentially the same as Eq. (5), except that we now use the density at the interface and we have a correspondingly different value for S_s. By using the density at the surface, we allow S_s to be independent of the device configuration and be more independent of the carrier density.

IV. SIMPLE MODEL FOR NONRADIATIVE LIFETIME

In this section, we derive a simplistic model for the density dependence of the nonradiative lifetime. Technically, this model is only valid for samples with a large active region, where the carrier densities stay constant across most of the active region with a very small depletion region near the junction. We label this case as wide-active-layer limit. The samples which we analyze here (with $d=1\ \mu$m or $d=0.75\ \mu$m) do not meet this criterion. However, even for these samples the simple model for the nonradiative lifetime is a useful tool for their characterization. We will not use this model in any other calculations, such as those for the cooling characteristics in Sec. VI. In that section, we will calculate the external quantum efficiency and cooling efficiency directly without resorting to the simple nonradiative lifetime model. The simple model, however, will be of great value for interpreting the results of Sec. VI.

We focus on the density dependence of the nonradiative recombination using Eq. (10). The S from Eq. (6) and S_s from (10) are related by:

Author complimentary copy. Redistribution subject to AIP license or copyright, see http://jap.aip.org/jap/copyright.jsp

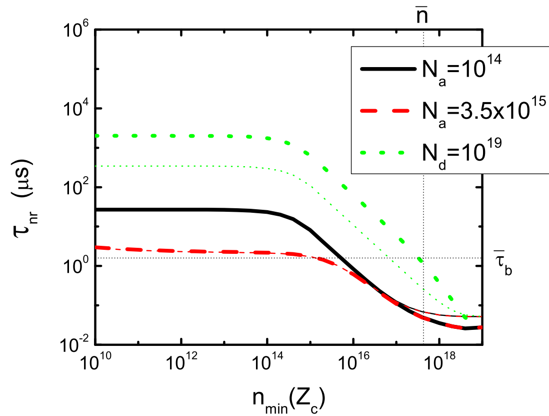

FIG. 2. (Color online) Density dependence of τ_{nr} for $T=300$ K. The thick lines are calculated using the $n_{\mathrm{min}}(Z_j)/n_{\mathrm{min}}(Z_c)$ ratios, whereas the thin lines are calculated using the $n_{\mathrm{min}}(Z_j-5\ \mathrm{nm})/n_{\mathrm{min}}(Z_c)$ ratios. The thin solid and dashed lines are indistinguishable from the corresponding thick lines. The solid and dashed lines, labeled $N_a=10^{14}$ and $N_a=3.5\times10^{15}$, respectively, are for structures with the GaAs p-doping indicated by N_a (units of per cubic centimeter) and an n-doping in the GaInP layer of $N_d=10^{17}\ \mathrm{cm}^{-3}$. The dotted curves show a structure with a GaAs p-doping of $N_a=10^{14}\ \mathrm{cm}^{-3}$ and a GaInP n-doping of $N_d=10^{19}$.

$$S=\frac{n_{\mathrm{min}}(Z_j)}{n_{\mathrm{min}}(Z_c)}S_s, \tag{11}$$

where $Z_c=0$ is the center of the heterostructure and Z_j is the position of the GaAs/GaInP junction.

In laser cooling analyses (e.g., Ref. 5) it is usually assumed that the nonradiative recombination stems primarily from the surface/interface recombination and the density is assumed to be constant across the structure's active layer such that

$$A=2\frac{S}{d}. \tag{12}$$

The nonradiative lifetime is given by the inverse of A,

$$\tau_{nr}=1/A. \tag{13}$$

In order to get a general feel for the effect of the heterostructure on laser cooling, we combine Eqs. (11)–(13) to get

$$\tau_{nr}=\frac{n_{\mathrm{min}}(Z_c)}{n_{\mathrm{min}}(Z_j)}\frac{d}{2S_s} \tag{14}$$

We note that Eq. (12) is not strictly valid if the density is not constant across the active region. This will be addressed in greater detail in Sec. V. Still, Eq. (14) provides useful insight into the effect of the heterostructure on nonradiative recombination.

There has been significant experimental laser cooling work on a sample with a 1 μm active region that has a measured nonradiative lifetime of 27 μs.[5] The lifetime was measured at low densities. As we discuss in Sec. V, we believe that the initial estimates of the acceptor concentration in Ref. 5 may have to be revised downward from $N_a=3.5\times10^{15}\ \mathrm{cm}^{-3}$ to approximately $N_a=10^{14}\ \mathrm{cm}^{-3}$, and we estimate the donor concentration in the passivation layers to be $N_d=10^{17}\ \mathrm{cm}^{-3}$. In Fig. 2, we show the expected density dependence for τ_{nr} for this sample. Assuming that S_s is independent of the doping densities, we also show the expected

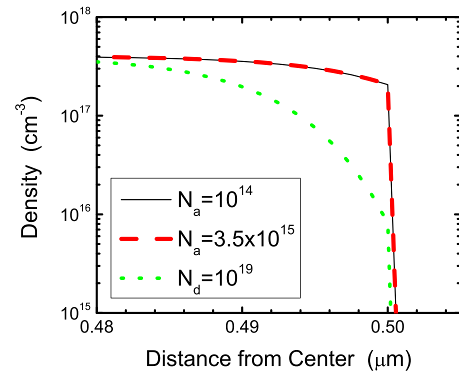

FIG. 3. (Color online) Hole density profile near the GaAs/GaInP junction for 300 K at $n_{\mathrm{min}}(Z_c)=4\times10^{17}$. For the solid and dashed lines $N_d=10^{17}\ \mathrm{cm}^{-3}$. For the dotted line, $N_a=10^{14}\ \mathrm{cm}^{-3}$. The active layer thickness $d=1.0\ \mu$m.

τ_{nr} for a rather high donor concentration of $N_d=10^{19}\ \mathrm{cm}^{-3}$ with an acceptor concentration of $N_a=10^{14}\ \mathrm{cm}^{-3}$.

For reference, the optimal cooling density ($\bar{n}=4.3\times10^{17}\ \mathrm{cm}^{-3}$) and break even nonradiative lifetime ($\bar{\tau}_b=1.6\ \mu$s) for 300K, calculated with the cooling theory for spatially homogeneous systems detailed in Refs. 13 and 14 (compare also Ref. 15) are also shown. We find that even though the sample under consideration has a nonradiative lifetime at low densities that is significantly above the break-even nonradiative lifetime, at the optimal cooling density the nonradiative lifetime is too small to achieve cooling. For p-doping of $N_a=3.5\times10^{15}\ \mathrm{cm}^{-3}$, the nonradiative lifetime is decreased for low densities,[16] but there is no significant change at higher densities. In order to increase the nonradiative lifetime at the optimal cooling density, the n-doping in the GaInP needs to be increased. As one can see from Fig. 2, a sample with $N_d=10^{19}\ \mathrm{cm}^{-3}$ comes close to meeting the break-even cooling condition at room temperature.

In the above analysis, the reduction in the interface recombination comes from reducing the minority carrier density (holes) exactly at the junction. Figure 3 shows the hole density around the junction for $n=4\times10^{17}\ \mathrm{cm}^{-3}$ and $T=300$ K. It can be seen that increasing the n-doping to $10^{19}\ \mathrm{cm}^{-3}$ decreases the surface recombination by creating a very small depletion region around the junction. However, this means that the density is decreasing rapidly near the junction. In our current model, only the carriers at the very edge of the junction contribute to the surface recombination. In a more realistic model, the wave function of the surface states would extend away from the junction, and any carriers with a wave function that overlaps the wave function of the surface states would have a chance of being involved in the surface recombination. Since the depletion region near the junction is so small at this density, this will limit the ability of the heterostructure to reduce surface recombination. To get a feel for how significant of an effect this might have we have calculated the expected value for τ_{nr} under the assumption that $S\approx n_{\mathrm{min}}(Z_c)/n_{\mathrm{min}}(Z_j-5\ \mathrm{nm})S_s$, shown as thin lines in Fig. 2. The heterostructure still appears to help reduce interface recombination.

It should also be pointed out that $N_d=10^{19}\ \mathrm{cm}^{-3}$ is a very high doping concentration. If we assume the Bohr ra-

Author complimentary copy. Redistribution subject to AIP license or copyright, see http://jap.aip.org/jap/copyright.jsp

dius for the donor sites to be around 10 nm, we can roughly approximate the density where the donor sites will start to overlap as $1/a_0^3$, which results in a density of 10^{18} cm^{-3}. A donor density of $N_d=10^{19}$ cm^{-3} would have significant donor site overlap and could easily have undesirable effects that are not included in our current theory. It is sufficient to say that our current theory predicts that a sample with $N_d=10^{19}$ cm^{-3} and $N_a=10^{14}$ cm^{-3} should be able to achieve cooling at room temperature. Even though our theory is not completely accurate at this doping density, testing samples with high n-doping may still be worth the effort.

V. LUMINESCENCE DECAY IN N-P-N HETEROSTRUCTURES

Luminescence lifetime measurements are frequently used to determine the radiative and nonradiative recombination coefficients. For a spatially homogeneous p-doped semiconductor (cf., Ref. 5)

$$\frac{\partial n_e}{\partial t} = -An_e - \eta_e B_{eh} n_e n_h - \eta_e B_{ea} n_e n_a - C n_e n_h^2. \tag{15}$$

At low densities ($n_e \ll N_a$), n_h is dominated by the ionization of acceptors and essentially becomes a constant and the Auger recombination becomes negligible. In this case, Eq. (15) can be solved analytically as $n_e(t)=n_0\exp(-t/\tau)$ with $1/\tau=1/\tau_{nr}+1/\tau_{rad}=A+\eta_e B_{eh} n_h+\eta_e B_{ea} n_a$. For this to be true, it is essential that n_h and n_a be constant in time and space, so that the luminescence ($\eta_e B_{eh} n_e n_h + \eta_e B_{ea} n_e n_a$) is directly proportional to n_e. This condition results in an exponential decay for n_e that can be directly observed in the luminescence decay.

In the n-p-n heterostructures at low densities, the carrier densities [$n_e(z)$ and $n_h(z)$] are not constant across the active region. This leads to difficulties in understanding the meaning of the lifetime measurements. It is, therefore, desirable to calculate the theoretical luminescence decay for the n-p-n structure. For this analysis, we assume that the quasithermalization across the structure (due to diffusion and drift currents) occurs quickly compared to the radiative and nonradiative recombination, such that the system is always in quasithermal equilibrium. At high temperatures this assumption is more reasonable than at low temperatures, where it is likely to break down. Under this assumption the average number of optically induced electrons (holes) is given by

$$\bar{n}_e^{\text{opt}} = \frac{1}{d}\int_{-Z_e}^{Z_e} dz\{n_e(z) - n_e^{\text{don}}(z)\}, \tag{16}$$

$$\bar{n}_h^{\text{opt}} = \frac{1}{d}\int_{-Z_e}^{Z_e} dz\{n_h(z) - n_h^{\text{acc}}(z)\}. \tag{17}$$

Due to total charge neutrality, $\bar{n}_e^{\text{opt}}=\bar{n}_h^{\text{opt}}$. See the Appendix for more details on why the average optical density is used for the rate equations.

We break the radiative recombination into the electron-hole and electron-acceptor components such that the radiative recombination rate is given by[17]

$$\left(\frac{\partial \bar{n}_e^{\text{opt}}}{\partial t}\right)_{\text{rad}} = \left(\frac{\partial \bar{n}_h^{\text{opt}}}{\partial t}\right)_{\text{rad}} = \frac{1}{d}\int_{-Z_j}^{Z_j} dz[\eta_e B_{eh} n_e(z) n_h(z) + \eta_e B_{ea} n_e(z) n_a(z)], \tag{18}$$

where we have assumed that the radiative recombination in the GaInP layer is negligible.

The nonradiative surface recombination is assumed to be a Shockley–Read–Hall process at the two interfaces. Neglecting the intrinsic carrier densities with respect to the actual densities due to doping and/or optical excitation at the interface, the rates can be parameterized approximately as (compare Ref. 11)

$$\left(\frac{\partial \bar{n}_e^{\text{opt}}}{\partial t}\right)_{\text{surface}} = \left(\frac{\partial \bar{n}_h^{\text{opt}}}{\partial t}\right)_{\text{surface}} = \frac{2S_s}{d}\frac{n_e(z_j) n_h(z_j)}{n_e(z_j)+n_e(z_j)}, \tag{19}$$

where the factor of 2 accounts for both surfaces, d is the thickness of the GaAs active layer, and S_s is defined in Sec. III.

The Auger recombination is given by:

$$\left(\frac{\partial \bar{n}_e^{\text{opt}}}{\partial t}\right)_{\text{Auger}} = \left(\frac{\partial \bar{n}_h^{\text{opt}}}{\partial t}\right)_{\text{Auger}} = \frac{1}{d}\int_{-Z_j}^{Z_j} dz \max\{C n_e(z) n_h^2(z), C n_e^2(z) n_h(z)\}. \tag{20}$$

If we calculate the state of the n-p-n heterostructure using the theory presented in Sec. II for several different densities, then we can calculate the time it takes to transition between densities as

$$\Delta t = \frac{\Delta n_e^{\text{opt}}}{\left(\frac{\partial n_e^{\text{opt}}}{\partial t}\right)_{\text{rad}} + \left(\frac{\partial n_e^{\text{opt}}}{\partial t}\right)_{\text{surface}} + \left(\frac{\partial n_e^{\text{opt}}}{\partial t}\right)_{\text{Auger}}}. \tag{21}$$

The luminescence is given by the radiative recombination rate in Eq. (18), which combined with the times calculated with Eq. (21) allows us to calculate the luminescence decay.

As we have shown in Fig. 5 of Ref. 18, the luminescence decay for a 1 μm thick sample with $N_a=3.5\times10^{15}$ cm^{-3} (corresponding to the one reported in Ref. 5) for $T=300$ K does not exhibit an exponential time behavior, not even at low densities (corresponding to times >100 μs. The corresponding carrier densities for this structure are shown in Fig. 4. From Fig. 4 we see that at moderate to low densities (10^{10} and 10^{15} cm^{-3} minority carrier density at the center), the holes are the majority carriers in the center of the active region, and the electrons are the majority carriers at the edge of the active region. In order to make the assumptions necessary to get an exponential luminescence decay, we need one of the carriers to be significantly larger then the other. This condition is not maintained across the active region, which results on a nonexponential luminescence decay (in the present case the decay is almost proportional to $t^{-1.2}$).

Figures 5 and 6 show the experimental luminescence decay measurements for a sample with similar doping concentrations to the sample in Ref. 5 with a 0.75 μm GaAs active region and 0.75 μm GaInP passivation

Author complimentary copy. Redistribution subject to AIP license or copyright, see http://jap.aip.org/jap/copyright.jsp

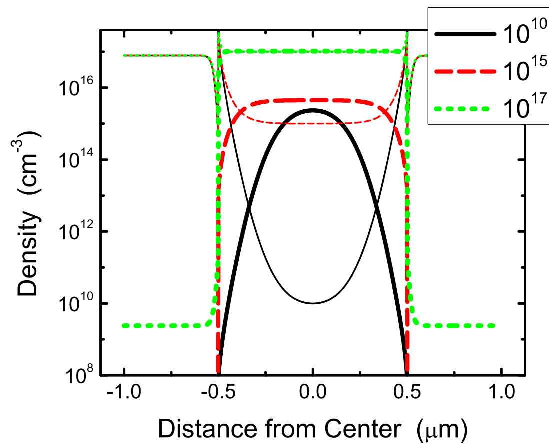

FIG. 4. (Color online) Carrier densities for a 1 μm thick sample with $N_a = 3.5 \times 10^{15}$ cm^{-3} and $N_d = 10^{17}$ cm^{-3} at 300 K. Electrons (thin lines) and holes (thick lines). The figure shows results for three different minority carrier densities at the center, indicated in units of per cubic centimeter in the figure.

layers. We find that we are able to obtain a reasonable match to this data if we assume $N_a = 10^{14}$ cm^{-3} and $S_s = 1000e^{-18\ \text{meV}/k_BT}$ cm/s. This sample was still mounted to a GaAs substrate. The $d = 1.0$ μm sample in Ref. 5 that was mounted to a GaAs substrate, was found to have a $S < 0.6$ cm/s at 300 K. With our calculations the $d = 0.75$ μm sample has $S_s = 499$ cm/s at 300K with $n_{\min}(Z_j)/n_{\min}(Z_c) = 0.001\ 83$, which results in $S = 0.91$ cm/s.

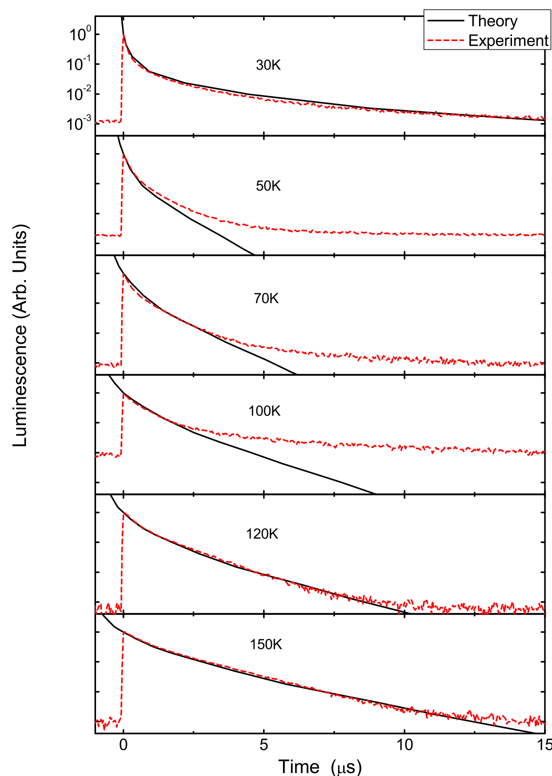

FIG. 5. (Color online) Luminescence decay for various temperatures from $T = 30$ K to $T = 150$ K, for a sample of GaAs layer thickness $d = 0.75$ μm. In the theoretical results (solid lines) the doping concentration is $N_a = 10^{14}$ cm^{-3} and $N_d = 10^{17}$ cm^{-3}. The experimental results are shown as dashed lines.

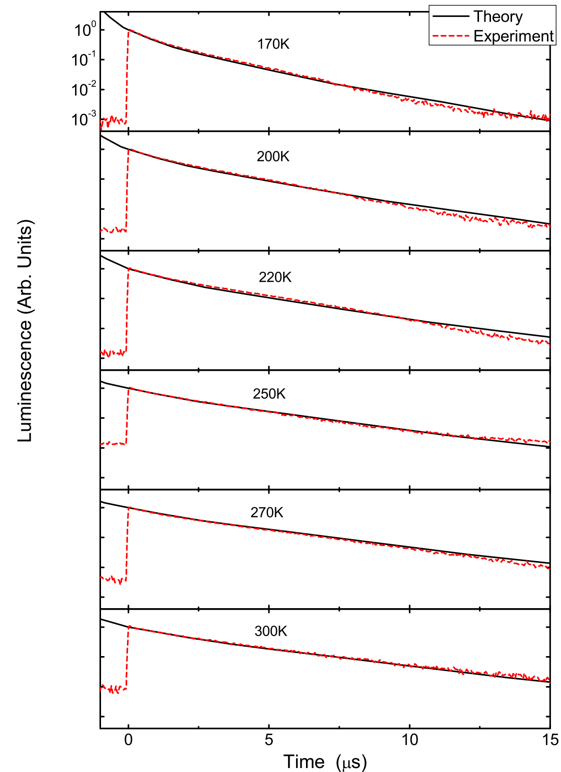

FIG. 6. (Color online) Same as Fig. 5 but for temperatures ranging from 170 to 300 K.

With the sample mounted to a GaAs substrate with unknown impurity concentration and nonradiative recombination, it is difficult to accurately calculate the extraction efficiency η_e, which is defined as the fraction of luminescence light that escapes from the sample.[19] To model η_e, we extended our luminescence theory in Ref. 20 to account for light propagation in and extraction from the active layer, details of which will be given in a forthcoming publication[21] (see also Ref. 22). We used that propagation model for a sample with a dome and adjusted the refractive index of the dome to match the experimental data. We found that a refractive index of $n_d = 1.9$ gave the best match to the experimental data. In addition, the experimental data have arbitrary luminescence units, which allows us to adjust the vertical scale to best match the data, and the starting density is unknown, which allows us to shift the time axis to best match the data.

At low temperatures (below 100 K) the theoretical model does not match the experimental data as well as we would like. There are several reasons not to expect our current theoretical model to work as well at low temperatures. First, as mentioned before, the assumption of quasithermal equilibrium may break down at low temperatures. Second, our current model for the n-p-n heterostructure uses a free (=noninteracting) carrier model to calculate the carrier densities. At low temperatures exciton formation and density dependent band-gap shift can create significant errors in the free carrier model. In addition, the current model uses the low density coefficients B_{eh} and B_{ea} as a constant across the sample. B_{eh} will decrease significantly as function of density if the density is high enough, which is especially significant at low temperatures (cf. Fig. 3 of Ref. 13). We believe that

Author complimentary copy. Redistribution subject to AIP license or copyright, see http://jap.aip.org/jap/copyright.jsp

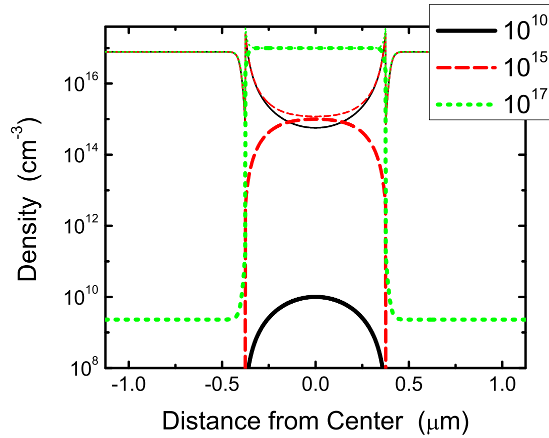

FIG. 7. (Color online) Carrier densities for a 0.75 μm thick sample with $N_a=10^{14}$ at 300 K. Electrons (thin lines), holes (thick lines). The figure shows results for three different minority carrier densities at the center, indicated in units of per cubic centimeter in the figure.

further improvements to the theory could result in a better quantitative fit to the experiment at low temperature but those quantitative improvements are not likely to affect the insight into the interface recombination in n-p-n structures gained from our present analysis.

Figure 7 shows the carrier densities in the sample with $N_a=10^{14}$ and a 0.75 μm thickness. In this case at moderate to low densities, the electrons are the majority carriers across the full active region. This appears to allow the luminescence to have an exponential decay. However, because the electrons are the majority carrier in the p-doped active region, instead of the holes, we must be careful in interpreting the results of the lifetime measurements. Assumptions such as $n_h \approx N_a$ and $n_e \ll n_h$ are clearly invalid for this structure (cf. Ref. 18).

VI. EFFECT OF HETEROSTRUCTURES ON COOLING

This section studies the effect of the heterostructure on the overall cooling. This analysis is done by looking at the cooling efficiency (the ratio of net cooling to input power),

$$\eta_c = \frac{-P_{\text{net}}}{P_{\text{in}}} = \eta_{\text{ext}} \frac{\omega_\ell}{\omega_a} \frac{\alpha(\omega_a)}{\alpha(\omega_a) + \alpha_b + \sigma_{\text{fca}} n} - 1. \tag{22}$$

Here, ω_ℓ and ω_a are the mean luminescence frequency and the optimal absorption frequency, respectively, $\alpha(\omega_a)$ is the absorption coefficient for the interband absorption, α_b accounts for parasitic background absorption, and σ_{fca} is the free-carrier absorption coefficient. All density-dependent quantities are to be evaluated at the optimal cooling density. Finally, the external quantum efficiency (η_{ext}) is the ratio of the number of photons out of the sample to the number of photons absorbed, and is calculated as

$$\eta_{\text{ext}} = \frac{\left(\frac{\partial \bar{n}_e^{\text{opt}}}{\partial t}\right)_{\text{rad}}}{\left(\frac{\partial \bar{n}_e^{\text{opt}}}{\partial t}\right)_{\text{surface}} + \left(\frac{\partial \bar{n}_e^{\text{opt}}}{\partial t}\right)_{\text{rad}} + \left(\frac{\partial \bar{n}_e^{\text{opt}}}{\partial t}\right)_{\text{Auger}}}. \tag{23}$$

η_{ext} can be estimated from experimental measurements, and measures how close a system is to achieving laser cooling.[23]

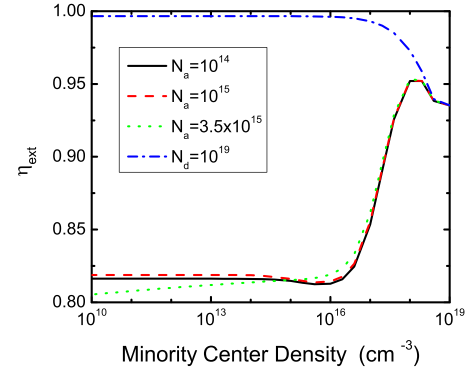

FIG. 8. (Color online) External quantum efficiency η_{ext} vs density at 300 K, for $d=1$ μm. By default $N_d=10^{17}$ cm^{-3}. For the dashed-dotted line $N_a=10^{14}$ cm^{-3} and $N_d=10^{19}$ cm^{-3}.

The optimal cooling density tends to be at moderately high densities where it is important to use a density dependent value for B_{eh}. In addition, since in the n-p-n structure we no longer have local charge neutrality, B_{eh} depends on both n_e and n_h. The extraction efficiency is also highly dependent on density, since higher densities decrease the photon reabsorption. In order to simplify these calculations, we approximate

$$\eta_e B_{eh}(n_e,n_h) \approx \eta_{e,\text{undoped}} B_{\text{undoped}}[\max(n_e,n_h)], \tag{24}$$

where $\eta_{e,\text{undoped}} B_{\text{undoped}}(n)$ is calculated using an homogeneous undoped semiconductor with the correct sample thickness and a ZnS dome.

The external quantum efficiency η_{ext} can be calculated using Eq. (24) in Eqs. (18)–(20) and (23). The results are shown in Fig. 8. The density dependence of η_{ext} can be understood by breaking it down to its individual components. The nonradiative, radiative, and Auger recombination rates for the $N_a=10^{14}$ cm^{-3} sample are shown in Fig. 9. For low densities, the electrons are the majority carriers, and are essentially independent of $n_{\min}(Z_c)$. This results in all of the recombination rates being directly proportional to $n_{\min}(Z_c)$, resulting in a constant η_{ext}.

For the range $3\times10^{14} < n_{\min}(Z_c) < 10^{17}$, $n_h(z)$ becomes similar in magnitude to $n_e(z)$. At this point, the radiative recombination takes on its normal $n_{\min}^2(Z_c)$ dependence, and the Auger recombination takes on its normal $n_{\min}^3(Z_c)$ dependence. The depletion region near the GaAs/GaInP junction

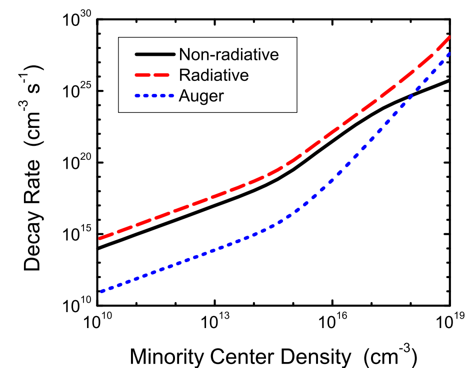

FIG. 9. (Color online) Breakdown of the density dependent decay rates for a sample with $d=1$ μm, $N_a=10^{14}$ cm^{-3}, $N_d=10^{17}$ cm^{-3} at 300 K.

Author complimentary copy. Redistribution subject to AIP license or copyright, see http://jap.aip.org/jap/copyright.jsp

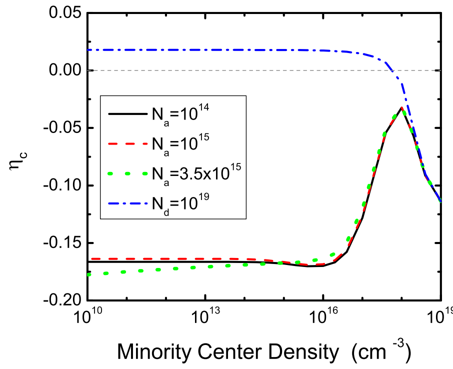

FIG. 10. (Color online) Cooling efficiency vs density at 300 K for $d=1$ μm. By default $N_d=10^{17}$ cm^{-3}. For the dashed-dotted line $N_a=10^{14}$ cm^{-3} and $N_d=10^{19}$ cm^{-3}.

starts to disappear causing the nonradiative recombination to increase faster then its normal $n_{\min}(Z_c)$ dependence. In this region the nonradiative recombination turns out to be approximately $\sim n_{\min}^2(Z_c)$. Which allows η_{ext} to remain almost constant through this region.

For the range $10^{17}<n_{\min}(Z_c)<10^{18}$, the depletion region has almost completely disappeared, so that $n_{\min}(Z_j)\approx n_{\min}(Z_c)$ causing the nonradiative recombination to go back to a $n_{\min}(Z_c)$ dependence. The radiative recombination increases faster then the nonradiative causing η_{ext} to increase.

For $n_{\min}>10^{18}$, the Auger recombination becomes greater then the nonradiative recombination and starts to reduce η_{ext}.

Finally, the cooling efficiency η_c can be calculated by plugging η_{ext} into Eq. (22). For this calculation, we approximate ω_ℓ, ω_a, and the ratio $(\alpha(\omega_a)/\alpha(\omega_a)+\alpha_b+\sigma_{\text{fca}}n)$ by the values for a homogeneous p-doped semiconductor with the same density as that at the center of the n-p-n structure. We have found that the absorption and luminescence is frequently a constant across the active region of the structure, and therefore approximating the structure's absorption and luminescence values by the corresponding values at the center of the structure should be reasonable.

The results for η_c are shown in Fig. 10. The two structures $N_a=10^{14}$ and $N_a=3.5\times10^{15}$, which both have $N_d=10^{17}$ cm^{-3}, show similar results. By adjusting the p-doping in this structure, we can increase or decrease the low density nonradiative recombination. Unfortunately, the radiative recombination is adjusted by a similar amount resulting in no improvement for the overall cooling. In the end, the cooling results for different p-doping concentrations are surprisingly similar. In contrast, increasing the n-doping [see the $N_d=10^{19}$ cm^{-3} (solid) line] decreases the nonradiative recombination without decreasing the radiative recombination. This allows the overall structure to achieve cooling with a positive η_c.

VII. CONCLUSION

In conclusion, we found that an n-p-n heterostructure can significantly reduce the surface recombination for low densities by reducing the minority carrier density near the interface. However, this effect only occurs for moderately low densities. At high densities, this effect disappears. Since the nonradiative lifetime is inherently measured at low densities, this can lead to the case where a sample has a good nonradiative lifetime but still has an unacceptable amount of nonradiative recombination at the optimal cooling density.

We believe that this effect has so far hindered laser cooling of semiconductor experiments at room temperature. The nonradiative lifetime in existing samples is an order of magnitude better then is required for laser cooling. However, at the optimal laser cooling density, the nonradiative recombination rate has increased dramatically and laser cooling may no longer be possible.

In order to propose a solution to the problem of the deterioration of the nonradiative decay at high densities, we have varied the doping in the n and p regions. We find that increasing the n-doping appears to improve (decrease) the nonradiative recombination rate for both low and high densities. If the n-doping can be increased sufficiently ($\approx 10^{19}$ cm^{-3}) without causing undesired side effects (such as "bleeding" of Si dopants from the n-region into the active layer), then we believe that it should be possible to create a sample where semiconductor laser cooling can be achieved at room temperature. Since laser cooling of semiconductors is expected to become easier as the temperature is decreased, there is no known reason why such a cooler could not reach cryogenic temperatures. We believe that our analysis presents a novel approach to the design and possible optimization of semiconductor structures intended for use in laser cooling.

ACKNOWLEDGMENTS

We thank B. Imangholi and M. Hasselbeck for helpful discussions. We acknowledge financial support from AFOSR (MURI Grant No. FA9550-04-1-0356), and additional support from JSOP. G.R. gratefully acknowledges financial support from TRIF.

APPENDIX: VARIABLES USED IN HETEROSTRUCTURE RATE EQUATIONS

For quasithermal equilibrium, we assume that the electrons in the conduction band and at the donor sites are in thermodynamic equilibrium with one chemical potential while the holes in the valence band and at the acceptor sites are in equilibrium with another chemical potential. The total number of electrons in the combined conduction band plus donor site system is given by

$$n_e^{\text{tot}}=\int_{-Z_e}^{Z_e} dz\{n_e(z)+[N_d(z)-N_d^+(z)]\}, \tag{A1}$$

and the total number of holes in the combined valence band plus acceptor site system is

$$n_h^{\text{tot}}=\int_{-Z_e}^{Z_e} dz\{n_h(z)+[N_a(z)-N_a^-(z)]\}. \tag{A2}$$

Rate equations can then be used to model the creation or annihilation of electrons in the conduction band-donor site system and the creation or annihilation of holes in the valence band-acceptor site system. Since electrons and holes

Author complimentary copy. Redistribution subject to AIP license or copyright, see http://jap.aip.org/jap/copyright.jsp

are always created or annihilated in pairs, $\partial n_e^{\mathrm{tot}}/\partial t = \partial n_h^{\mathrm{tot}}/\partial t$. We separate the holes in the valence band according to whether they were due to optical excitation or acceptor ionization such that $n_e(z) = n_e^{\mathrm{opt}}(z) + n_e^{\mathrm{don}}(z)$, $n_h(z) = n_h^{\mathrm{opt}}(z) + n_h^{\mathrm{acc}}(z)$, where $n_e^{\mathrm{don}}(z) = N_d^+(z)$ and $n_h^{\mathrm{acc}}(z) = N_a^-(z)$. Solving for the optical component and integrating across the structure, we have

$$n_e^{\mathrm{opt}} = \int_{-Z_e}^{Z_e} dz[n_e(z) - n_e^{\mathrm{don}}(z)], \tag{A3}$$

$$n_h^{\mathrm{opt}} = \int_{-Z_e}^{Z_e} dz[n_h(z) - n_h^{\mathrm{acc}}(z)]. \tag{A4}$$

We note that $n_e^{\mathrm{opt}}(n_h^{\mathrm{opt}})$ is related to $n_e^{\mathrm{tot}}(n_h^{\mathrm{tot}})$ by a constant:

$$n_e^{\mathrm{opt}} = n_e^{\mathrm{tot}} - \int_{-Z_e}^{Z_e} dz N_d(z), \tag{A5}$$

$$n_h^{\mathrm{opt}} = n_h^{\mathrm{tot}} - \int_{-Z_e}^{Z_e} dz N_a(z). \tag{A6}$$

This results in $\partial n_e^{\mathrm{opt}}/\partial t = \partial n_e^{\mathrm{tot}}/\partial t = \partial n_h^{\mathrm{opt}}/\partial t = \partial n_h^{\mathrm{tot}}/\partial t$. Due to total charge neutrality we have

$$\int_{-Z_e}^{Z_e} dz\{[n_e(z) - N_d^+(z)] - [n_h(z) - N_a^-(z)]\} = 0, \tag{A7}$$

which can be re-written as

$$\int_{-Z_e}^{Z_e} dz\{n_e^{\mathrm{opt}}(z) - n_h^{\mathrm{opt}}(z)\} = 0, \tag{A8}$$

from which $n_e^{\mathrm{opt}} = n_h^{\mathrm{opt}}$ follows. In order to keep the density in units of per cubic centimeter, we define an average optical density $\bar{n}_e^{\mathrm{opt}} = n_e^{\mathrm{opt}}/d = \bar{n}_h^{\mathrm{opt}} = n_h^{\mathrm{opt}}/d$ We use these variables for the n-p-n heterostructure rate equations in Sec. V.

[1] M. Sheik-Bahae and R. I. Epstein, Laser Photonics Rev. **3**, 67 (2009).
[2] M. Sheik-Bahae and R. I. Epstein, *Optical Refrigeration* (Wiley, New York, 2009).
[3] G. Nemova and R. Kashyap, Rep. Prog. Phys. **73**, 086501 (2010).
[4] D. V. Seletskiy, S. D. Melgaard, S. Bigotta, A. DiLieto, M. Tonelli, and M. Sheik-Bahae, Nat. Photonics **4**, 161 (2010).
[5] B. Imangholi, M. P. Hasselbeck, M. Sheik-Bahae, R. I. Epstein, and S. Kurtz, Appl. Phys. Lett. **86**, 081104 (2005).
[6] R. K. Ahrenkiel, D. J. Dunlavy, B. Keyes, S. M. Vernon, T. M. Dixon, S. P. Tobin, K. L. Miller, and R. E. Hayes, Appl. Phys. Lett. **55**, 1088 (1989).
[7] N. W. Ashcroft and N. D. Mermin, *Solid State Physics* (Sounders College, New York, 1976).
[8] $m_e = 0.13 m_0$ for GaP (p. 5828 of Ref. 10) and $m_e = 0.0795 m_0$ for InP (p. 5829 of Ref. 10) resulting in $m_e = 1.05 m_0$ for $Ga_{51}In_{49}P$ by linear interpolation.
[9] $m_h = 0.67 m_0$ for GaP (Ref. 24) and $m_h = 0.56$ for InP (Ref. 24) resulting in $m_h = 0.62 m_0$ for $Ga_{51}In_{49}P$ by linear interpolation.
[10] I. Vurgaftman, J. R. Meyer, and L. R. Ram-Mohan, J. Appl. Phys. **89**, 5815 (2001).
[11] X. Correig, J. Calderer, E. Blasco, and R. Alcubilla, Solid-State Electron. **33**, 477 (1990).
[12] B. Adamowicz and H. Hasegawa, Jpn. J. Appl. Phys., Part 1 **37**, 1631 (1998).
[13] G. Rupper, N. H. Kwong, and R. Binder, Phys. Rev. B **76**, 245203 (2007).
[14] G. Rupper, N. H. Kwong, B. Gu, and R. Binder, *Laser Refrigeration of Solids* (SPIE, Bellingham, WA, 2008), Vol. 6907, p. 690705.
[15] J. Khurgin, J. Appl. Phys. **100**, 113116 (2006).
[16] For a p-doping of $N_a = 10^{14}$ cm^{-3}, the electrons are the center minority carrier. As the p-doping is increased, the low density lifetime initially increases. Eventually, the center minority carrier becomes the holes, and then the low density lifetime decreases as the p-doping is increased.
[17] In the GaInP layers, $n_h(z)$ is very small. This results in almost no radiative recombination from these layers. Rather then calculate B_{eh} and B_{dh} for GaInP, we ignore the tiny amount of radiative recombination that comes from the GaInP layers.
[18] G. Rupper, N. H. Kwong, and R. Binder, *Laser Refrigeration of Solids III* (SPIE, Bellingham, WA, 2010), Vol. 7614, p. 76140D.
[19] M. Sheik-Bahae and R. I. Epstein, Phys. Rev. Lett. **92**, 247403 (2004).
[20] N. H. Kwong, G. Rupper, and R. Binder, Phys. Rev. B **79**, 155205 (2009).
[21] N. H. Kwong, G. Rupper, and R. Binder, 2009 (unpublished).
[22] G. Rupper, Ph.D. thesis, University of Arizona, 2010.
[23] M. Sheik-Bahae, B. Imangholi, M. P. Hasselbeck, R. I. Epstein, and S. Kurtz, *Advances in Laser Cooling of Semiconductors* (SPIE, Bellingham, WA, 2006), Vol. 6115, p. 611518.
[24] *Semiconductors Basic Data*, edited by O. Madelung (Springer, Berlin, 1996), pp. 93–126.

Author complimentary copy. Redistribution subject to AIP license or copyright, see http://jap.aip.org/jap/copyright.jsp